Title

Dopamine receptor D_4 (DRD_4) polymorphisms with reduced functional potency intensify atrophy in syndrome-specific sites of frontotemporal dementia.

Authors

Butler, PM
Chiong, W
Perry, DC
et al.

Publication Date

2019

DOI

10.1016/j.nicl.2019.101822

Peer reviewed

NeuroImage: Clinical 23 (2019) 101822

Contents lists available at ScienceDirect

NeuroImage: Clinical

journal homepage: www.elsevier.com/locate/ynicl

Dopamine receptor D_4 (*DRD*$_4$) polymorphisms with reduced functional potency intensify atrophy in syndrome-specific sites of frontotemporal dementia

P.M. Butler[a,*], W. Chiong[a], D.C. Perry[a], Z.A. Miller[a], E.D. Gennatas[a], J.A. Brown[a], L. Pasquini[a], A. Karydas[a], D. Dokuru[b], G. Coppola[b], V.E. Sturm[a], A.L. Boxer[a], M.L. Gorno-Tempini[a], H.J. Rosen[a], J.H. Kramer[a], B.L. Miller[a], W.W. Seeley[a]

[a] Department of Neurology, Memory and Aging Center, University of California San Francisco, San Francisco, CA, USA
[b] Departments of Psychiatry and Neurology, Semel Institute for Neuroscience and Human Behavior, David Geffen School of Medicine, University of California at Los Angeles, Los Angeles, CA, USA

ARTICLE INFO

Keywords:
Frontotemporal dementia
DRD$_4$
Apathy
Insula
Anterior cingulate cortex
Salience network

ABSTRACT

Objective: We aimed to understand the impact of dopamine receptor D_4 (*DRD*$_4$) polymorphisms on neurodegeneration in patients with dementia. We hypothesized that *DRD*$_4$ *dampened-variants* with reduced functional potency would be associated with greater atrophy in regions with higher receptor density. Given that *DRD*$_4$ is concentrated in anterior regions of the limbic and cortical forebrain we anticipated genotype effects in patients with a more rostral pattern of neurodegeneration.

Methods: 337 subjects, including healthy controls, patients with Alzheimer's disease (AD) and frontotemporal dementia (FTD) underwent genotyping, structural MRI, and cognitive/behavioral testing. We conducted whole-brain voxel-based morphometry to examine the relationship between *DRD*$_4$ genotypes and brain atrophy patterns within and across groups. General linear modeling was used to evaluate relationships between genotype and cognitive/behavioral measures.

Results: *DRD*$_4$ dampened-variants predicted gray matter atrophy in disease-specific regions of FTD in anterior cingulate, ventromedial prefrontal, orbitofrontal and insular cortices on the right greater than the left. Genotype predicted greater apathy and repetitive motor disturbance in patients with FTD. These results covaried with frontoinsular cortical atrophy. Peak atrophy patterned along regions of neuroanatomic vulnerability in FTD-spectrum disorders. In AD subjects and controls, genotype did not impact gray matter intensity.

Conclusions: We conclude that *DRD*$_4$ polymorphisms with reduced functional potency exacerbate neuronal injury in sites of higher receptor density, which intersect with syndrome-specific regions undergoing neurodegeneration in FTD.

1. Introduction

Each neurodegenerative disease exhibits phenotypic diversity with regard to clinical manifestations and neuroanatomical injury patterns (Seeley, 2017). Considerable attention has been given to genes related to the etiopathogenesis of neurodegeneration (Chow et al., 1999; Goldman et al., 2005), but the genes that impact phenotypic diversity are poorly understood.

In the first investigations of this kind, researchers have identified several genes that modify the neuroanatomical phenotype. Gennatas

Abbreviations: *DRD*$_4$, Dopamine receptor D_4; AD, Alzheimer's disease; FTD, Frontotemporal dementia; *COMT*, Catechol-*O*-methyltransferase; *ApoE4*, Apolipoprotein ε4; VNTR, Variable number tandem repeat; cAMP, Cyclic adenosine monophosphate; bvFTD, Behavioral variant frontotemporal dementia; svPPA, Semantic variant primary progressive aphasia; nfvPPA, Non-fluent/agrammatic variant primary progressive aphasia; CBS, Corticobasal syndrome; PSP, Progressive supranuclear palsy; MMSE, Mini-Mental State Examination; CVLT, California Verbal Learning Test; BNT, Boston Naming Test; CDR, Clinical Dementia Rating Scale; NPI, Neuropsychiatric Inventory; PCR, Polymerase chain reaction; SPM, Statistical parametric mapping; MNI, Montreal Neurological Institute; FWHM, Full-width at half-maximum; VBM, Voxel-based morphometry; FWE, Family-wise error; AI, Anterior insula; ACC, Anterior cingulate cortex; vmPFC, Ventromedial prefrontal cortex; OFC, Orbitofrontal cortex; dmPFC, Dorsomedial prefrontal cortex

* Corresponding author at: 675 Nelson Rising Lane, Suite 190, San Francisco, California 94158, USA.
E-mail address: Monroe.Butler@ucsf.edu (P.M. Butler).

https://doi.org/10.1016/j.nicl.2019.101822
Received 16 April 2018; Received in revised form 4 April 2019; Accepted 9 April 2019
Available online 10 April 2019

et al. (2012) demonstrated that the Val^{158}Met polymorphism in the catechol-*O*-methyltransferase (*COMT*) gene influences neurodegeneration in a dose-dependent fashion such that *COMT* polymorphisms associated with increased synaptic dopamine catabolism predicted focal atrophy in the ventral tegmental area, ventral striatum, insula, and ventromedial prefrontal cortex (vmPFC). Functional polymorphisms in the language-associated *FOXP2* gene are associated with decreased perfusion of the left inferior frontal region and reduced verbal fluency in frontotemporal dementia (FTD) patients (Padovani et al., 2010). Dyslexia susceptibility genes, *KIAA0319* and *CNTNAP2*, are associated with cortical thinning in left frontoinsular sites in FTD (Paternico et al., 2016). Agosta et al. (2009) showed that the apolipoprotein ε4 (*ApoE4*) genotype correlated with worsened atrophy in disease-specific regions in both Alzheimer's disease (AD) and FTD. This finding helped stimulate studies showing that *ApoE4* worsens neurodegeneration in mouse models of primary tauopathy (Shi et al., 2017). This assortment of studies suggests that genetic variation is important to understand neuroanatomical phenotypes in neurodegeneration. In particular, findings from Gennatas et al. (2012) suggest that change in metabolic efficiency related to *COMT* polymorphisms can aggravate cellular stress and impact neurodegeneration. Interestingly, while *COMT* functions to inactivate several neurotransmitters across the brain, Val^{158}Met polymorphisms exert a focal pattern of neurodegeneration centered on high-density sites of dopaminergic activity. It remains uncertain whether receptor-level bioenergetics within dopamine systems play a role in neurodegeneration.

The human dopamine receptor D_4 (*DRD_4*) gene, located near the telomere of chromosome *11p* in humans, is highly polymorphic with much of the variation due to the length of a 48-base pair tandem repeat (VNTR) in exon 3, which encodes the third cytoplasmic loop of the receptor (Lichter et al., 1993; Wang et al., 2004). Alleles with 2–11 repeats have been described, but the three most common variants (4R, 2R, and 7R alleles) explain over 90% of the population diversity (Ding et al., 2002). Polymorphisms alter the intracellular loop structure, and subsequently the downstream neuronal signaling (Asghari et al., 1995; Oak et al., 2000), while receptor-level dopamine binding profiles are relatively similar across allelic variants (Asghari et al., 1994). 2R and 7R variants lead to blunted second messenger response. Compared to 4R/4R (wild-type) receptor function, dopamine potency to inhibit cyclic adenosine monophosphate (cAMP) production is decreased by 30–40% in 2R variants and 70–80% in 7R transfected cells (Asghari et al., 1995). Less is known about the functional potency for other uncommon variants (e.g. 3R, 5R, 6R, 8R).

DRD_4 expression across the brain is variable, with higher receptor densities in anterior regions of the limbic and cortical forebrain (Lahti et al., 1998; Matsumoto et al., 1995). This anterior pattern is reflected in the data which demonstrate variation in receptor-level function impacts executive and behavioral regulation (Gatt et al., 2015; Munafò et al., 2008; Rondou et al., 2010). Here, we questioned whether the common 2R- and 7R-variants would influence neurodegeneration, behavior, and cognition in a cross-sectional group of aged patients with and without neurodegenerative disease. Reduced efficiency of inhibitory second-messenger signaling presumably incites downstream cellular stress in sites previously vulnerable to neurodegeneration. Subjects with common allelic variants (2R, 4R, and 7R) were included for analysis based on a priori hypotheses related to receptor-level effects of genotype and to minimize the confounding effects of alleles with unknown downstream neuronal function (Rondou et al., 2010). We hypothesized that *DRD_4 dampened-variants* (2R and 7R) with reduced functional potency would be associated with greater atrophy in regions with higher *DRD_4* receptor density, especially in patients with a more rostral pattern of neurodegeneration.

2. Methods

2.1. Subjects

We queried the University of California San Francisco (UCSF) Memory and Aging Center database for subjects who had undergone *DRD_4* genotyping, brain structural MRI, and cognitive/behavioral testing. Subjects included were those deemed cognitively normal or meeting clinical criteria for a diagnosis of dementia based on published consensus research criteria for AD or an FTD-spectrum disorder (Armstrong et al., 2013; Gorno-Tempini et al., 2011; Litvan et al., 1996; McKhann et al., 2011; Neary et al., 1998). FTD-spectrum diagnoses included behavioral variant frontotemporal dementia (bvFTD), semantic variant primary progressive aphasia (svPPA), non-fluent/agrammatic variant primary progressive aphasia (nfvPPA), corticobasal syndrome (CBS), and progressive supranuclear palsy (PSP). Participants underwent behavioral and cognitive testing within 1 year of neuroimaging and clinical diagnoses. Earliest initial evaluations were included for all subjects followed longitudinally. Neuropathology was confirmed in 98 of 207 patients with dementia. Age-matched controls were free from neuropsychiatric history and did not take psychotropic medications except for 1 individual who reported using trazodone as needed for sleep. In dementia patients, there was 1 patient with CBS on levodopa/carbidopa for treatment of parkinsonian motor symptoms and 5 patients with bvFTD on scheduled or as-needed anti-psychotics for varying reasons (1 each on aripiprazole, olanzapine, risperidone, and 2 on quetiapine). Procedures were approved by the UCSF Committee on Human Research. All subjects and/or caretakers provided informed consent prior to study participation. All data was collected between the years of 2000 to 2017. Demographic information was compared with unpaired two-tailed *t*-tests and Pearson χ^2 tests.

2.2. Cognitive and behavioral testing

Neuropsychological batteries included in bedside screening protocols have been described in prior publications (see Rosen et al., 2002). To summarize briefly, global cognitive function was assessed with the Mini-Mental State Examination (MMSE). Verbal episodic memory was tested with the California Verbal Learning Test (CVLT) 9-item short form. Visual episodic memory was measured with 10-min free recall of the Benson figure, and figure copy was utilized for visuospatial assessment. Language evaluation included the 15-item Boston Naming Test (BNT), phonemic and semantic fluency. Tests of executive function included digit-span backwards, Stroop testing, and a modified Trails B test. Global function and disease severity were assessed by the Clinical Dementia Rating (CDR) scale and the CDR sum-of-boxes score. Behavioral symptoms were measured by the Neuropsychiatric Inventory (NPI). Test scores nearest to the date of neuroimaging were included in the analysis. 188 of 207 patients (90.8%) underwent imaging within 90 days of clinical evaluations and 202 of 207 patients (97.6%) within 6 months (mean = 27.6 days, SD = 46.5, interquartile range 2–38).

2.3. *DRD_4* genotyping

The *DRD_4* exon 3 VNTR was assayed by polymerase chain reaction (PCR) testing with the AccuPrime™ Taq High Fidelity DNA Polymerase kit. The reaction contained a 6-FAM labeled forward primer (/56-FAM/GCGACTACGTGGTCTACTCG) and a reverse primer (AGGACCCTCATGGCCTTG), as described in Lichter et al. (1993). PCR reactions were submitted for fragment analysis on an AB3730XL with a LIZ1200 size standard. This method is a modification of the gel-based assay reported by Chen et al. (1999). 2R, 4R, and 7R alleles represented 92.4% of all alleles in our sample, which is similar to known allele frequencies (Butler and Matthews, 2011; Ding et al., 2002). Allele frequencies and genotypes by group were compared with Pearson χ^2 tests.

2.4. Image acquisition

Structural brain MRIs were acquired on one of three scanners. 152 subjects were scanned at the San Francisco Veteran's Administration Hospital on a 1.5-Tesla Magnetom VISION system (Siemens, Iselin, NJ) using a standard quadrature head coil. A volumetric magnetization prepared rapid gradient-echo MRI (MPRAGE, TR/TE/TI = 10/4/300 ms) was used to obtain T1-weighted images of the entire brain with 15° flip angle, coronal orientation perpendicular to the double spin-echo sequence, 1.0 × 1.0 mm in-plane resolution and 1.5 mm slab thickness. Another 85 participants underwent imaging at the UCSF Neuroscience Imaging Center on a 3-Tesla Siemens (Siemens, Iselin, NJ) TIM Trio scanner equipped with a 12-channel head coil. T-1 weighted MPRAGE images were obtained (TR/TE/TI = 2300/2.98/900 ms) with 9° flip angle. The field of view was 240 × 256 mm, with 1 × 1 mm in-plane resolution and 1 mm slice thickness. The remaining 100 scans were performed at the San Francisco Veteran's Administration Hospital on a 4-Tesla (Bruker/Siemens; Bruker BioSpin MRI GmbH, Ettlingen, Germany) MRI system with a birdcage transmit and 8-channel receive coil. T1-weighted MPRAGE sequences (TR/TE/TI = 2300/3/950 ms) were acquired with 7° flip angle and 1.0 × 1.0 × 1.0 mm^3 resolution. Scanner type was controlled for in linear models as a nuisance covariate.

2.5. Image preprocessing

Scans were visually inspected for artifact. 1 subject was excluded for excessive motion artifact but a subsequent repeat scan was adequate for inclusion. SPM12 (http://www.fil.ion.ucl.ac.uk/spm/) was utilized for data preprocessing, which included segmentation into gray matter, white matter, and CSF and then alignment and normalization to Montreal Neurological Institute (MNI) space. Modulation and smoothing with an 8-mm full-width at half-maximum (FWHM) Gaussian kernel was applied. Total intracranial volume was computed by SPM12 through an automated estimation process to integrate and sum voxel values from gray matter, white matter, and CSF. Preprocessed images were assessed for quality with the *check sample homogeneity* function in CAT12 (http://dbm.neuro.uni-jena.de/cat/), which is an SPM12 extension toolbox. In all preprocessing steps, default parameters were utilized. The final voxel resolution was 1.5 mm × 1.5 mm × 1.5 mm (3.375 mm^3).

2.6. Statistical analysis

Voxel-based morphometry (VBM) was performed with statistical parametric mapping techniques. Smoothed gray matter maps were entered into a general linear model with group (control, AD, FTD) as a factor and genotype as the covariate-of-interest. Genotype was modeled on a linear, interval scale from 1 to 3 for the 4R, 2R, and 7R groups, which reflected proportional, step-wise loss-of-potency as previously described (Asghari et al., 1995). The 4R group was defined by the wild-type (4R/4R genotype). The 2R group was composed of the 2R/4R and 2R/2R genotypes. 4R/7R, 7R/7R, and 2R/7R genotypes defined the 7R group. Nuisance covariates included age-at-scan, sex, total intracranial volume (TIV), scanner type, and CDR sum-of-boxes. Absolute threshold masking was set at 0.1. For comparisons within dementia patients, we utilized proportional scaling (subject-level global normalization per image) to control for confounding effects of differing severity in global atrophy within these heterogeneous dementing illnesses (Ridgway et al., 2009). Statistical maps were initially examined at a level of $p_{uncorr} < 0.001$ uncorrected for multiple comparisons. The threshold for statistical significance was set at $p_{FWE\text{-}corr} < 0.05$ after family-wise error (FWE) correction for multiple comparisons (Nichols and Holmes, 2002). Given that *DRD$_4$* receptors are present in varying densities throughout the brain, then whole-brain VBM was preferred to regionally masked analyses (Callier et al., 2003).

Prior to testing our primary hypotheses about impact of *DRD$_4$* dampened function on neurodegeneration, we first performed a confirmatory analysis to demonstrate patterns of gray matter atrophy in patients and controls after controlling for age-at-scan, sex, scanner type, and TIV. SPM *t*-tests compared whole-brain gray matter maps of controls vs. AD, controls vs. FTD, and AD vs. FTD. Two models were employed to test for relationships between genotype and gray matter intensity maps. First, we assessed for the effect of *DRD$_4$* genotype across all subjects controlling for nuisance predictors, including diagnostic group with dummy variable coding. We tested for effects of polymorphisms across all subjects because the impact of *DRD$_4$* dampened function on aging is relatively unknown and because previous findings from dopamine system genes (e.g. *COMT*) showed polymorphism effects across aged subjects, although results were driven primarily by dementia patients (Gennatas et al., 2012). To specifically test our hypothesis that dampened *DRD$_4$* function exacerbates neurodegeneration in patients with a more rostral pattern of atrophy, we modeled diagnostic group (e.g. healthy control, AD, FTD) as a categorical variable and genotype as the covariate-of-interest, which included interaction effects with diagnostic group. Nuisance covariates were age-at-scan, sex, TIV, scanner type, and disease severity (e.g., CDR sum-of-boxes).

General linear models were used to evaluate relationships among *DRD$_4$* genotype, neuropsychological performance, and NPI scores in dementia patients. These analyses were performed in STATA 15.0 (StataCorp LLC). NPI sub-scores were only analyzed when at least 50% of patients within a diagnostic group had non-zero results. NPI scores and cognitive scores served as dependent variables in separate regression models. Cases with missing data were excluded list-wise. In the models for cognitive and behavioral data, diagnosis (AD or FTD) was a fixed factor and *DRD$_4$* genotype was the covariate-of-interest, which was modeled in the same fashion as in the imaging analyses. Nuisance covariates included age-at-scan, sex, TIV, education, and CDR sum-of-boxes score. *P*-values < 0.05 were considered significant after controlling for multiple comparisons.

The results from primary hypothesis testing led to two second-order VBM analyses to better understand the relationships between genotype, behavior, and FTD-spectrum syndromes. Significant NPI sub-scores predicted by *DRD$_4$* dampened-variants in FTD were used as covariates-of-interest in SPM *T*-contrast tests, which masked findings by regions identified from primary hypothesis testing. In another model, we tested for interactions between FTD-specific syndromes and genotype after controlling for typical nuisance parameters.

3. Results

3.1. Demographic, genetic, behavioral, and cognitive data

Table 1 displays basic demographic and genetic characteristics by group. *Supplemental Table 1* displays genotype and allele frequency data by group. Patients and controls did not differ by age, education, allele frequencies or genotype. Dementia patients did not differ in male-to-female ratio, however the ratios differed between patients and controls, which were controlled for in all statistical models. Compared to age-matched controls, patients with dementia were impaired on global cognitive measures (MMSE) without difference between patients with AD versus FTD. FTD patients were more clinically impaired than those with AD based on CDR scores. Within FTD, *DRD$_4$* dampened-variants were more clinically impaired than wild-types. Given these differences, we controlled for disease severity with CDR sum-of-boxes score as covariate in linear models.

FTD-spectrum diagnoses and demographics are listed in *Supplemental Table 2*. 104 FTD patients were composed of: 50 bvFTD, 26 svPPA, 16 CBS, 7 nfvPPA, and 5 PSP. 56 of 104 patients with clinical FTD syndromes were later confirmed neuropathologically to have frontotemporal lobar degeneration (FTLD). More specifically, 26 bvFTD, 13 svPPA, 9 CBS, 5 nfvPPA, and 3 PSP patients were

Table 1
Subject characteristics

	Control		AD		FTD	
	4R/4R	2R + 7R	4R/4R	2R + 7R	4R/4R	2R + 7R
Subjects, N	85	45	64	39	65	39
Age-at-scan	64.5 (9.4)	64.6 (9.4)	65.6 (10.3)	66.2 (10.9)	62.9 (9.2)	62.0 (8.7)
Sex, M:F	31:54†*	13:32†*	38:26†	22:17†	38:27*‡	15:24*‡
Education	16.9 (2.5)	16.8 (2.0)	16.0 (3.3)	15.9 (3.2)	15.2 (3.1)	15.6 (2.8)
Illness Duration	–	–	4.8 (2.3)	4.6 (2.1)	5.4 (4.3)	5.1 (2.9)
CDR, Total	–	–	0.9 (0.5)‡	0.9 (0.4)‡	0.9 (0.7)‡∂	1.3 (0.7)‡∂
CDR, sum-of-boxes	–	–	4.6 (3.2)‡	4.8 (2.2)‡	5.2 (3.6)‡∂	6.8 (3.7)‡∂
MMSE (max = 30)	29.3 (0.8)◊	29.6 (0.6)◊	21.8 (6.6)◊	21.8 (6.1)◊	23.5 (6.8)◊	22.6 (6.6)◊
Allele Frequency, %	71.2	16.9 + 11.9	70.4	16.5 + 13.1	70.0	18.0 + 12.0

Abbreviations: CDR = clinical dementia scale, MMSE = Mini-Mental State Exam, M = male, F = female, AD = Alzheimer's disease, FTD = frontotemporal dementia. Age-at-scan, education, and illness duration are listed in years.
Statistically significant comparisons: There was a significant difference in male-to-female ratios in controls compared to AD ($\chi^2 = 13.9$, $p = 0.0002^{\dagger}$) and FTD ($\chi^2 = 6.9$, $p = 0.008^{*}$). Within the FTD group males-to-female ratios differed between 4R/4R wild-and those with 2R and 7R ($\chi^2 = 3.90$, $p = 0.048^{\ddagger}$). AD ($t = 14.2$, $p = 0.0001$) and FTD ($t = 11.0$, $p = 0.0001^{\diamond}$) patients were significantly impaired on MMSE testing compared to controls. FTD compared to AD patients were more impaired based on the CDR ($t = 2.36$, $p = 0.02$) and CDR sum-of-boxes score ($t = 2.38$, $p = 0.02^{\ddagger}$). Within the FTD group the 2R and 7R group were more clinically impaired on CDR ($t = 2.82$, $p = 0.006^{\partial}$) and CDR sum-of-boxes ($t = 2.17$, $p = 0.03$) compared to the wild-type 4R/4R.
Statistically insignificant comparisons: Subjects did not differ by group in age or education ($ps > 0.05$), genotype ($\chi^2 = 5.18$, $p = 0.74$) allele frequencies ($\chi^2 = 0.102$, $p = 0.99$), or by genotype grouping (e.g., 4R vs 2R vs 7R groups, $\chi^2 = 1.36$, $p = 0.85$). AD and FTD subjects did not differ by illness duration ($t = 1.37$, $p = 0.17$), MMSE scores (ps > 0.1), and male-to-female ratios ($\chi^2 = 1.11$, $p = 0.29$).

pathologically proven to be FTLD. 42 of 103 patients with a clinical diagnosis of probable AD were later neuropathologically confirmed at autopsy. No patients with a clinical diagnosis of an FTD-spectrum disorder were found to have a non-FTLD primary neuropathological diagnosis, and no patients with clinical AD were found to have a non-AD primary neuropathological diagnosis.

Table 2 demonstrates the NPI scores in AD and FTD patients by genotype groups. General linear modeling demonstrated worsened NPI apathy sub-scores were predicted by interaction effect between *DRD$_4$* dampened-variants and FTD ($t = 2.03$, $p = 0.04$). There was a trend toward significance with higher NPI repetitive motor disturbance sub-scores being predicted by interaction effect between *DRD$_4$* dampened function and FTD ($t = 1.65$, $p = 0.099$). Cognitive outcome variables were not predicted by interaction effects between diagnosis and genotype after controlling for multiple comparisons. *Supplemental table 4* lists results from the neuropsychological battery.

3.2. Neuroimaging analyses

Fig. 1 shows atrophy patterns for AD compared to controls, FTD compared to controls, and FTD compared to AD. Patients with AD demonstrated greater posterior than anterior brain atrophy with peak gray matter loss in the posterior cingulate cortex, precuneus, mesial temporal cortex, and lateral temporoparietal cortex. Patients with FTD exhibited greater anterior than posterior atrophy with accentuated gray matter loss in the anterior insula (AI), anterior cingulate cortex (ACC), anterior and inferior temporal cortex, vmPFC, and orbitofrontal cortex (OFC). A rostral pattern of atrophy distinguished patients with FTD compared to AD.

Table 2
NPI scores in dementia patients by DRD$_4$ genotype.

NPI Scores	Alzheimer's Dementia			Frontotemporal Dementia		
	4R	2R	7R	4R	2R	7R
Apathy	3.92 (4.1)	4.3 (3.6)	2.8 (3.1)	5.5 (4.4)	7.4 (3.7)**	7.5 (4.8)**
Eating	1.6 (2.5)	1.8 (3.3)	2.6 (3.0)	4.4 (4.5)	5.1 (4.3)	5.0 (3.8)
Disinhibition	1.8 (3.8)	1.3 (2.4)	0.5 (1.2)	4.2 (4.3)	2.6 (2.6)	4.9 (4.6)
Irritability	2.2 (3.0)	2.3 (2.8)	1.9 (3.0)	2.2 (3.4)	2.6 (2.6)	2.0 (3.8)
Motor	1.9 (3.4)	1.2 (2.1)	1.5 (3.4)	3.8 (4.5)	7.1 (4.4)*	5.9 (5.4)*
NPI Total	19.8 (17.8)	18.4 (21.4)	18.3 (16.0)	28.8 (22.0)	38.8 (15.5)	40.7 (29.6)

** Denotes statistical significance with $p < 0.05$
* denotes a trend toward significance with $p < 0.10$. The relationship to NPI Total score was not significant ($t = 1.47$, $p = 0.14$). Other sub-scores examined were non-significant ($p > 0.2$).

DRD$_4$ dampened function did not predict differences in gray matter intensity maps across all subjects when controlling for diagnostic group. In testing our primary hypothesis that *DRD$_4$* dampened-variants predicted atrophy in patients with a more rostral pattern of neurodegeneration, we modeled diagnosis as a factor and assessed for interaction with genotype. There was significant interaction effect between the FTD group and *DRD$_4$* dampened function (7R > 2R > 4R). Fig. 2 displays statistical parametric maps with regions of decreased gray matter intensity in FTD predicted by interaction effects with genotype. *DRD$_4$* dampened-variants predicted atrophy in the right AI, bilateral (right > left) ventral and dorsal ACC, right vmPFC, and right OFC. Findings are embedded within the atrophy maps from FTD compared to controls. Table 3 lists results from Fig. 2 with peak *T*-values and coordinates in Montreal Neurological Institute (MNI) space. Interaction effects between genotype and group did not predict differences in gray matter intensity maps in AD patients or controls.

To understand the neuroanatomical correlates of behavioral change, NPI sub-scores for apathy and repetitive motor behavior were included as covariates-of-interest in separate VBM analyses, which modeled diagnostic group as a categorical variable and controlled for all nuisance parameters. Results were masked by those regions identified in the primary analysis (see Fig. 2 and Table 3) with greater atrophy associated with *DRD$_4$* dampened function. Fig. 3 displays the SPM *T*-contrasts with significantly decreased gray matter signal within areas predicted by *DRD$_4$* dampened-function, which correlated with the NPI sub-scores for apathy and repetitive behavior. Results are overlaid on regional atrophy in FTD related to worsened apathy and repetitive behavior irrespective of genotype. Worsened apathy NPI sub-scores in FTD predicted decreased gray matter intensity within regions associated with *DRD$_4$* dampened function, including the right AI, right mid-insula, right OFC, right subgenual and ventral ACC, and left ventral ACC. The significant right insular cluster contained 516 voxels with a peak *T*-value of 5.16 in the right inferior AI at MNI-coordinates *30/21/−15*. The right OFC cluster contained 1418 voxels with peak *T*-value of 4.59 at MNI-coordinates *8/32/−27*. A smaller cluster of 206 voxels was identified in the left ventral ACC with peak *T*-value of 4.12 at *−8/45/*

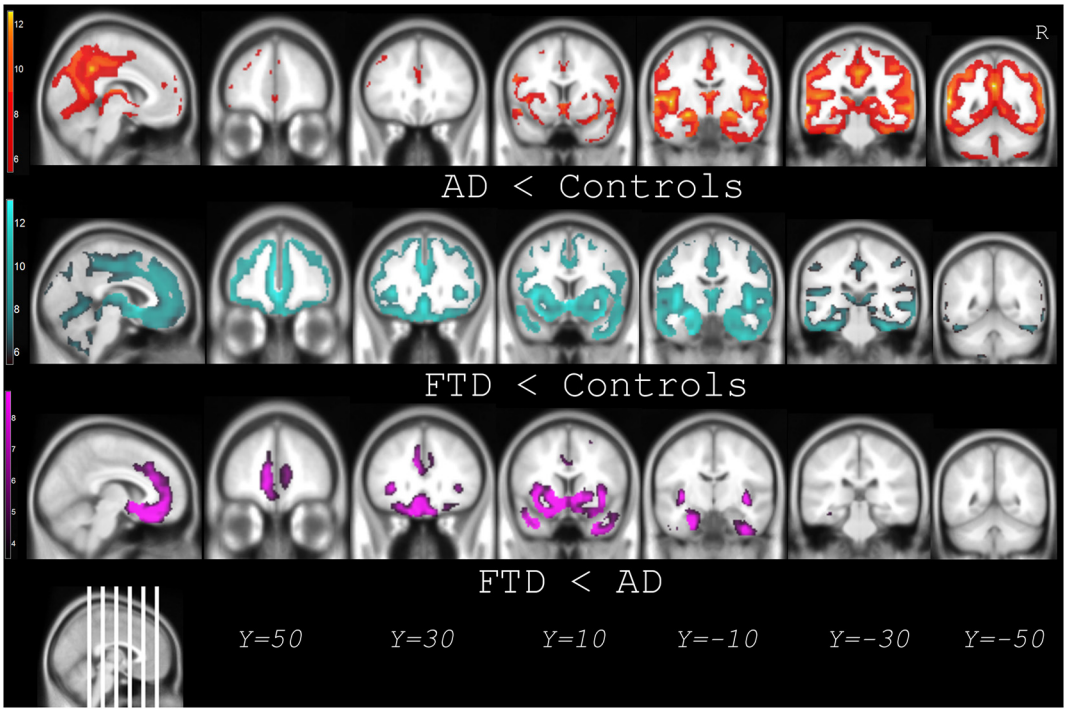

Fig. 1. Global atrophy patterns between dementia patients and age-matched controls.
VBM analyses controlling for age, sex, scanner type, and total intracranial volume confirmed the AD and FTD diagnostic groups exhibited atrophy patterns that were consistent with their clinical syndromes. Statistical parametric maps were corrected at $p_{\text{FWE-corr}} < 0.05$. $N = 337$. Results are displayed on a coronal MNI slice-labeled average template brain.

15 in MNI-space. Worsened NPI sub-scores for repetitive motor behavior in FTD predicted decreased gray matter intensity within regions associated with *DRD₄* dampened function, including the right insula and ventral ACC. Within the right insula there were 530 voxels with peak *T*-value of 5.56 in the right mid-insula with MNI-coordinates *34/10/−4*. The right ventral ACC showed a significant cluster of 665 voxels peak *T*-value of 4.06 at *8/46/2* in MNI-space.

To evaluate possible syndrome-specific effects, FTD-spectrum diagnoses of bvFTD ($N = 50$) and svPPA ($N = 26$) were coded as distinct groups in the categorical variable for diagnosis in SPM modeling. The other FTD syndrome groups were underpowered to detect meaningful group-level differences by genotype and were subsequently excluded from this analysis. We performed whole-brain gray matter contrasts by group with genotype as the covariate-of-interest and controlled for nuisance parameters as before. Fig. 4 displays the syndrome-specific atrophy effects of *DRD₄* polymorphisms within bvFTD and svPPA. Table 4 lists the MNI-coordinates and neuroanatomical regions of decreased gray matter intensity that covaried with *DRD₄* polymorphisms in bvFTD and svPPA. In bvFTD, there was notable decrease in right anterior and mid-insula, right ventral ACC/OFC, and right anterior and inferior temporal sites. In svPPA, *DRD₄* dampened-variants predicted atrophy in bilateral superior dorsolateral PFC, dorsomedial prefrontal cortex (dmPFC), and bilateral dorsal ACC/vmPFC.

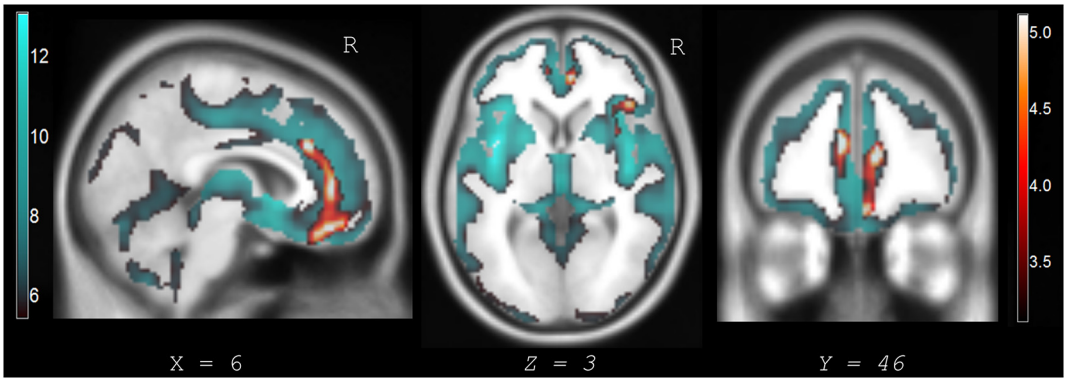

Fig. 2. Regions where DRD_4 dampened function is associated with greater atrophy in FTD with results nested in FTD versus control atrophy maps.
Interaction effect by group and genotype showed significant clusters of decreased gray matter intensity in FTD patients predicted by *DRD₄* dampened-variants. VBM analyses controlled for age, sex, scanner type, total intracranial volume, and disease severity (CDR sum-of-boxes). Corrected statistical parametric maps are displayed at $p_{\text{FWE-corr}} < 0.05$. Significant results are displayed with the orange/red heat map and embedded in larger regional atrophy maps from FTD compared to controls, which is displayed with the blue/green color map. Slices are labeled with MNI coordinates. Results are overlaid on an MNI average template brain. Interaction effects by genotype and group in AD and controls were not significant predictors of gray matter intensity change. Table 3 lists the MNI coordinates of significant voxels/clusters in FTD predicted by interaction effects with *DRD₄* dampened-variants.

Table 3
Decreased gray matter intensity signals in FTD predicted by interaction effects between diagnostic group and DRD_4 polymorphisms with dampened function.

Anatomic region	MNI Coordinates			Peak *T*-value	Cluster Size
	X	Y	Z		
Right ventral ACC/vmPFC	10	44	10	5.24	
Right dorsal ACC/dmPFC	8	28	28	4.60	2178
Right ventral ACC/medial OFC	4	42	−20	4.29	
Right anterior insula	27	22	−15	4.51	
Right lateral OFC	42	27	2	4.19	720
Right mid-insula	38	−4	9	3.87	
Left ventral ACC	−8	45	16	4.45	299

Abbreviations: MNI = Montreal Neurologic Institute coordinate space, ACC = anterior cingulate cortex, vmPFC = ventromedial prefrontal cortex, dmPFC = dorsal medial prefrontal cortex, OFC = orbitofrontal cortex. Cluster size is listed at the voxel-level (voxel size is 1.5 mm^3). Results are significant at $p_{FWE\text{-}corr} < 0.05$.

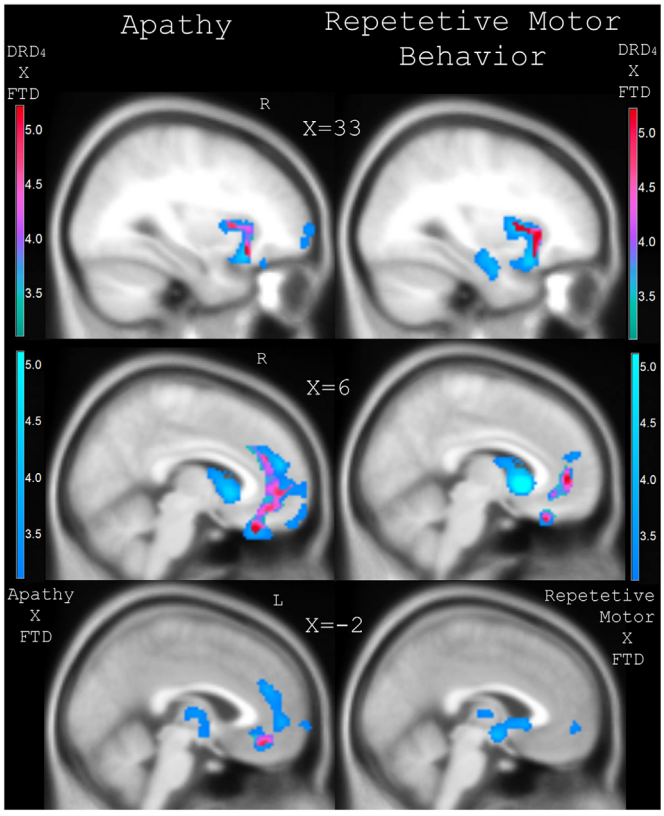

Fig. 3. Regional atrophy in FTD correlated with worsened apathy and repetitive motor behavior which covaried with decreased gray matter signal predicted by DRD_4 dampened function.
Statistical parametric maps of significantly decreased gray matter intensities which were predicted by interaction effect between FTD group and NPI apathy and repetitive motor sub-scores. Results were masked by regions of atrophy related to *DRD4* dampened function. Results are displayed at $p_{FWE\text{-}corr} < 0.05$ with red/purple heat maps embedded in blue maps which denote regions of significant atrophy related to worsened apathy and repetitive motor behavior in all patients with FTD. Results are overlaid on an MNI average template brain. Coronal slices are labeled with MNI coordinates.

4. Discussion

The substantial anatomical and clinical heterogeneity within dementia syndromes influences diagnostic certainty and prognosis (Perry et al., 2017). Identifying sources of patient-level variation is important to clarify disease mechanisms and suggest possible targets for patient-tailored disease-modifying therapies. Building on previous findings (Agosta et al., 2009; Gennatas et al., 2012; Padovani et al., 2010) the present research supports the hypothesis that an individual's background genetic constitution impacts the manifestation of neurodegenerative illness. Beyond disease susceptibility effects, genotype can shape the spatial landscape of degeneration and associated cognitive and behavioral profiles.

Previous work demonstrates that *DRD4* dampened-variants exhibit linearly reduced receptor-level potency in second-messenger response (Asghari et al., 1995). In the present study, we asked whether these variants known to impact downstream signaling fidelity might exacerbate neuronal injury in regions of high-receptor density. Results supported our hypothesis, as *DRD4* dampened-variants displayed accentuated atrophy in the right AI, dorsal and ventral ACC, vmPFC, and OFC. Rostral cortical degeneration, rather than posterior or striatal, was predicted by genotype in patients with FTD.

DRD4 dampened-variants with FTD exhibited greater behavioral apathy. Worsened NPI apathy sub-scores covaried with decreased gray matter signals predicted by *DRD4* dampened-function in the right anterior-inferior insula, right OFC, and right greater than left ventral ACC. While repetitive motor behavior only demonstrated a trend toward significance in general linear modeling of NPI sub-scores, the SPM *T*-map contrasts showed significant patterns of signal change predicted by *DRD4* dampened function in FTD subjects in the right AI, mid-insula and ventral ACC. In terms of overall clinical severity, patients with FTD in the 2R and 7R groups compared to the 4R wild-type group were more clinically impaired based on CDR scores. This potential confound could be due to chance variation in our cross-sectional sample (e.g. ascertainment bias) or it could reflect *DRD4*-mediated effects. To control for this possible confound, measures of clinical severity were used as predictors in linear models.

We evaluated the correlates of *DRD4* polymorphisms within bvFTD and svPPA, the two FTD syndromes with sufficient sample size to detect syndrome-specific patterns. Atrophy was intensified in right ventral frontotemporal structures in bvFTD and bilateral dorsal frontal sites in svPPA. More specifically, in bvFTD *DRD4* dampened-variants predicted gray matter density loss in right AI, mid-insula, right inferior and anterior temporal cortex, and right ventral ACC/OFC. In svPPA, polymorphisms correlated with bilateral superior frontal, dmPFC and vmPFC/ACC. In bvFTD, *DRD4*-associated atrophy within the right insula nested within well-described foci of atrophy. In svPPA, on the other hand, atrophy involved syndrome-related sites but not the peak hubs of atrophy (e.g. left anterior/inferior temporal cortex). Taken together, regionally aggravated degeneration in FTD patients under the influence of potency-reducing *DRD4* polymorphisms overlapped with key nodes of the salience network (Seeley et al., 2007). This large-scale brain network is selectively vulnerable in FTD, and has been shown to be involved in various forms of salience processing that modulate emotions, reward and homeostatic regulation (Guo et al., 2016; Seeley et al., 2009; Sturm et al., 2013). The localization of D_4 receptors to limbic and cortical systems of the anterior more than posterior forebrain might explain why patients with FTD but not AD dementia were susceptible to aggravated neurodegeneration in these regions. In other words, the neuronal milieu may be threatened most in regions of neuroanatomical overlap between typical sites of neurodegeneration and circuits richly innervated by D_4 receptors. FTD-spectrum disorders are associated with hypo-dopaminergic states (Huey et al., 2006), which taken together with *DRD4* dampened function might expose these rostral circuits to dysregulation thereby hastening degeneration.

How molecular pathophysiology translates into local and large-scale network degeneration remains unclear (Raj et al., 2012; Seeley et al., 2009; Warren et al., 2013; Zhou et al., 2012). Elucidating mechanistic links between *DRD4* circuit function and FTD-specific proteinopathies (e.g. TDP-43, tau) will be important for understanding how *DRD4* dampened-variants influence neurodegeneration. We tested the

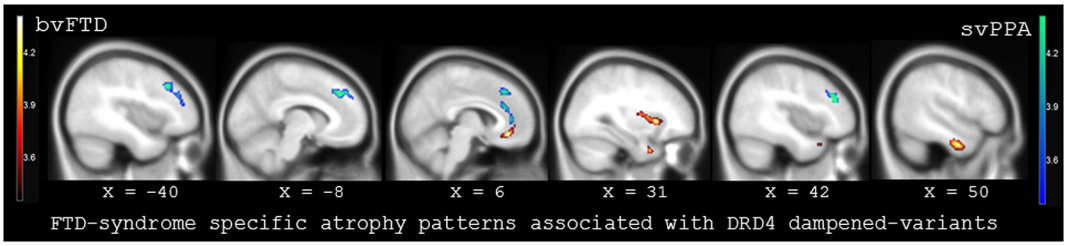

Fig. 4. Syndrome-specific atrophy in FTD related to DRD_4 dampened function.
50 patients with bvFTD (yellow/orange heat maps) and 26 with svPPA (green/blue maps) showed intensified atrophy associated with *DRD_4* polymorphisms. Corrected maps are displayed at $p_{FWE\text{-}corr} < 0.05$. Results are overlaid on an MNI average template brain. Slices are labeled with MNI coordinates. Table 4 displays the MNI coordinates to attain significance by interaction effect between FTD-syndromic diagnosis and *DRD_4* dampened function.

Table 4
FTD-syndrome specific atrophy in bvFTD and svPPA predicted by interaction effect between diagnosis and genotype.

FTD-spectrum diagnosis	Anatomic region	MNI Coordinates			Peak *T*-value	Cluster Size
		X	Y	Z		
bvFTD	Right anterior/mid-insula	32	18	2	4.30	461
	Right ventral ACC/OFC	4	36	−12	4.22	305
	Right inferior temporal	50	−4	−33	4.14	552
	Right anterior temporal	34	10	−34	4.13	241
svPPA	Right superior frontal	44	34	28	5.12	214
	Right dorsal ACC/vmPFC	9	34	22	4.80	455
	Left dmPFC	−8	38	39	4.78	328
	Right dmPFC	8	34	44	4.59	276
	Left superior frontal	−39	26	38	4.42	300

Abbreviations: MNI = Montreal Neurologic Institute coordinate space, ACC = anterior cingulate cortex, vmPFC = ventromedial prefrontal cortex, dmPFC = dorsomedial prefrontal cortex, and OFC = orbitofrontal cortex. Cluster size is listed at the voxel-level (voxel size is 1.5 mm^3). Results are significant at $p_{FWE\text{-}corr} < 0.05$.

hypothesis that decreased receptor efficiency (7R > 2R > 4R) in terms of second-messenger response to dopaminergic binding might mediate these effects. Even though modeled results of decreased regional gray matter intensity linearly covaried with D_4 dampened-variants in the expected fashion, the results might be driven by other mechanisms. The effects of D_4 receptor variants is not limited to the primary effects of functional potency of G-protein mediated cAMP response and might include release of inflammatory mediators (e.g. arachidonic acid), modulation of ion-channel currents, direct effects from SH3-domain binding, altered mRNA expression, altered receptor dimerization, antagonistic effects from other catecholamine systems, or dysregulation of corticostriatal glutamatergic projections (Mei et al., 1995; Oldenhof et al., 1998; Piomelli et al., 1991; Rondou et al., 2010; Tarazi and Baldessarini, 1999). The present findings raise the question of whether interaction effects might be present between *DRD_4* dampened-variants and COMT Val^{158}Met polymorphisms (Gennatas et al., 2012) in patients with dementia. Insufficient shared samples sizes precluded the possibility of probing for these interactions. Future investigations with bolstered sample sizes might consider interaction effects between polymorphic dopamine system genes, relationship between *DRD_4*-dampened function and familial forms of FTD (e.g. MAPT), and influence of polymorphisms on atypical parkinsonian disorders.

Clarifying the mechanisms whereby D_4 variants influence neurodegeneration is important when considering possible targets for patient-centered disease-modifying therapies. Studies investigating neuronal response to D_4-selective pharmacologic agents (e.g. agonist/antagonists) suggest there may be differential response in non-wild types (van Van Tol et al., 1992). Preferential localization of D_4 receptors in limbic/cortical more than striatal sites makes this target attractive for development of novel psychopharmacologic agents since animal models suggest decreased risk of extrapyramidal side effects (Yan et al., 2012).

Small sample sizes within several FTD-spectrum disorders (e.g. nfvPPA) limited the present study's ability to understand the influence of *DRD_4* polymorphisms on neurodegeneration within varying FTD clinical syndromes. Additionally, sample size may have been insufficient to detect small differences in cognitive measures within patient groups based on genotype. Behavioral correlates of *DRD_4*-dampened function in patients with FTD-spectrum disorders deserve further exploration with reward-processing and decision-making paradigms. Specific mechanistic hypotheses could be tested given *DRD_4* expression is high in frontal and insular cortices and relatively low in the shell of the nucleus accumbens (Svingos et al., 2000).

5. Conclusions

This study provides evidence that non-wild type *DRD_4* polymorphisms associated with blunted neuronal signaling predict decreased gray matter signal intensities in FTD within receptor-dense regions. Future studies should aim to understand longitudinal neuroanatomical and behavioral effects, network-based correlates, and possible serum or spinal fluid markers of neuronal injury. The human findings reported here could also serve as motivation for exploring the influence of manipulating dopamine signaling on FTD-related neurodegeneration in model organisms.

Acknowledgements

We thank contributors who collected samples used in this study, as well as patients and their families whose help and participation made this work possible. This work was supported by grants from the National Institute of Aging (T32 grant AG 23481-13 to P.M.B.), the National Institute of Health (P50 AG023501 and P01 AG019724 to H.J.R. and B.J.M), and the John Douglas French Alzheimer's Foundation (RC1 AG035610, R01 AG26938, R01 MH097268, and NS062691 to G.C). Samples from the National Cell Repository for Alzheimer's Disease (NCRAD), which receives government support under a cooperative agreement grant (U24 AG021886) awarded by the

National Institute on Aging (NIA), were used in this study. The authors declare no conflicts of interest.

Appendix A. Supplementary data

Supplementary data to this article can be found online at https://doi.org/10.1016/j.nicl.2019.101822.

References

Agosta, F., Vossel, K.A., Miller, B.L., Migliaccio, R., Bonasera, S.J., Filippi, M., Boxer, A.L., Karydas, A., Possin, K.L., Gorno-Tempini, M.L., 2009. Apolipoprotein E E4 is associated with disease-specific effects on brain atrophy in Alzheimer's disease and frontotemporal dementia. Proc. Natl. Acad. Sci. U. S. A. 106, 2018–2022.

Armstrong, M.J., Litvan, I., Lang, A.E., Bak, T.H., Bhatia, K.P., Borroni, B., Boxer, A.L., Dickson, D.W., Grossman, M., Hallett, M., Josephs, K., Kerterz, A., Lee, S.E., Miller, B.L., Reich, S.G., Riley, D.E., Tolosa, E., Tröster, A.I., Vidailhet, M., Weiner, W.J., 2013. Criteria for the diagnosis of corticobasal degeneration. Neurology 80, 496–503.

Asghari, V., Schoots, O., Van Kats, S., Ohara, K., Jovanovic, V., Guan, H.-C., Bunzow, J.R., Petronis, A., Van Tol, H.H.M., 1994. Dopamine D4 receptor repeat: analysis of different native and mutant forms of the human and rat genes. Mol. Pharm. 46, 364–373.

Asghari, V., Sanyal, S., Buchwaldt, S., Paterson, A., Jovanovic, V., Van Tol, H.H.M., 1995. Modulation of intercellular cyclic AMP levels by different human dopamine receptor variants. J. Neurochem. 65, 1157–1165.

Butler, P.M., Matthews, L.J., 2011. Novelty-seeking DRD4 polymorphisms are associated with human migration distance out-of-Africa after controlling for neutral population gene structure. Am. J. Phys. Anthr. 145, 382–389.

Callier, S., Snapyan, M., LeCrom, S., Prou, D., Vincent, J.D., Vernier, P., 2003. Evolution and cell biology of dopamine receptors in vertebrates. Biol. Cell. 95, 489–502.

Chen, C., Burton, M., Greenberger, E., Dmitrieva, J., 1999. Population migration and the variation of dopamine D4 receptor (DRD4) allele frequencies around the globe. Evol. Hum. Behav. 20, 309–324.

Chow, T.W., Miller, B.L., Hayashi, V.N., Geschwind, D.H., 1999. Inheritance of frontotemporal dementia. Arch. Neurol. 56, 817–822.

Ding, Y.-C., Chi, H.-C., Grady, D.L., Marishima, A., Kidd, J.R., Kidd, K.K., Flodman, P., Spence, M.A., Schuck, S., Swanson, J.M., Zhang, Y.-P., Moyzis, R.K., 2002. Evidence of positive selection acting at the human dopamine receptor D4 gene locus. Proc. Natl. Acad. Sci. U. S. A. 99, 309–314.

Gatt, J.M., Lurton, K.L.O., Williams, L.M., Schofield, P.R., 2015. Specific and common genes implicated across major mental disorders: a review of meta-analysis studies. J. Psychiatr. Res. 60, 1–13.

Gennatas, E.D., Cholfin, J.A., Zhou, J., Crawford, R.K., Sasaki, D.A., Karydas, A., Boxer, A.L., Bonasera, S.J., Rankin, K.P., Gorno-Tempini, M.L., Rosen, H,.J., Kramer, J.H., Weiner, M., Miller, B.L., Seeley, W.W., 2012. COMT Val^{158}Met genotype influences neurodegeneration within dopamine innervated brain structures. Neurology. 78, 1663–1669.

Goldman, J.S., Farmer, J.M., Wood, E.M., Johnson, J.K., Boxer, A., Neuhaus, J., Lomen-Hoerth, C., Wilhelmsen, K.C., Lee, V.M., Grossman, M., Miller, B.L., 2005. Comparison of family histories in FTLD subtypes and related tauopathies. Neurology. 65, 1817–1819.

Gorno-Tempini, M.L., Hillis, A.E., Weintraub, S., Kertesz, A., Mendez, M., Cappa, S.F., Ogar, J.M., Rohrer, J.D., Black, S., Boeve, B.F., Manes, F., Dronkers, N.F., Vandenberghe, R., Rascovsky, K., Patterson, K., Miller, B.L., Knopman, D.S., Hodges, J.R., Mesulam, M.M., Grossman, M., 2011. Classification of primary progressive aphasia and its variants. Neurology. 76, 1006–1014.

Guo, C.C., Sturm, V.E., Zhou, J., Gennatas, E.D., Trujillo, A.J., Hua, A.Y., Crawford, R., Stables, L., Kramer, J.H., Rankin, K., Levenson, R.W., Rosen, H.J., Miller, B.L., Seeley, W.W., 2016. Dominant hemisphere lateralization of cortical parasympathetic control as revealed by frontotemporal dementia. Proc. Natl. Acad. Sci. U. S. A. 113, E2430–E2439.

Huey, E.D., Putnam, K.T., Grafman, J., 2006. A systematic review of neurotransmitter deficitis and treatments in frontotemporal dementia. Neurology 66, 17–22.

Lahti, R.A., Roberts, R.C., Cochrane, E.V., Primus, R.J., Gallager, D.W., Conley, R.R., Tamminga, C.A., 1998. Direct determination of dopamine D4 receptors in normal and schizophrenic postmortem brain tissue: a [3H]NGD-94-1 study. Mol. Psychol. 3, 528:533.

Lichter, J.B., Barr, C.L., Kennedy, J.L., Van Tol, H.H.M., Kidd, K.K., Livak, K.J., 1993. A hypervariable segment in the human dopamine receptor D4 (DRD4) gene. Hum. Mol. Genet. 2, 767–773.

Litvan, I., Calne, A.Y., Campbell, G., Dubois, B., Duvoisin, R.C., Goetz, C.G., Golbe, L.I., Grafman, J., Growdon, J.H., Hallett, M., Jankovic, J., Quinn, N.P., Tolosa, E., Zee, D.S., 1996. Clinical research criteria for the diagnosis of progressive supranuclear palsy (Steele-Richardson-Olszewski syndrome): report of the NINDS-SPSP international workshop. Neurology. 47, 1–9.

Matsumoto, M., Hidaka, K., Tada, S., Tasaki, Y., Yamaguchi, T., 1995. Full-length cDNA cloning and distribution of human dopamine D4 receptor. Mol. Brain Res. 29, 157–162.

McKhann, G.M., Knopman, D.S., Chertkow, H., Hyman, B.T., Jack, C.R., Kawas, C.H., Klunk, W.E., Koroshetz, W.J., Manly, J.J., Mayeux, R., Mohs, R.C., Morris, J.C., Rossor, M.N., Scheltens, P., Carrillo, M.C., Thies, B., Weintraub, S., Phelps, C.H., 2011. The diagnosis of dementia due to Alzheimer's disease: recommendations from the National Institute on Aging-Alzheimer's Association workgroups on diagnostic guideline for Alzheimer's disease. Alzheimers Dement. 7, 263–269.

Mei, Y.A., Griffon, N., Buquet, C., Martres, M.P., Vaudry, H., Schwartz, J.-C., Sokoloff, P., Cazin, L., 1995. Activation of dopamine D_4 receptor inhibits an L-type calcium current in cerebellar granule cells. Neurosci. 68, 107–116.

Munafò, M.R., Yalcin, B., Willis-Owen, S.A., Flint, J., 2008. Association of the dopamine D4 receptor (DRD_4) gene and approach-related personality traits: meta-analysis and new data. Biol. Psychiatry 63, 197–206.

Neary, D., Snowden, J.S., Gustafson, L., Passant, U., Stuss, D., Black, S., Freedman, M., Kertesz, A., Robert, P.H., Albert, M., Boone, K., Miller, B.L., Cummings, J., Benson, D.F., 1998. Frontotemporal lobar degeneration: a consensus on clinical diagnostic criteria. Neurology 51, 1546–1554.

Nichols, T.E., Holmes, A.P., 2002. Nonparametric permutation tests for functional neuroimaging: a primer with examples. Hum. Brain Mapp. 15, 1–25.

Oak, J.N., Oldenhof, J., Van Tol, H.H.M., 2000. The dopamine D4 receptor: one decade of research. Eur. J. Pharmacol. 404, 303–327.

Oldenhof, J., Vickery, R., Anafi, M., Oak, J., Ray, A., Schoots, A., Schoots, O., Pawson, T., von Zastrow, M., Van Tol, H.H.M., 1998. SH3 binding domains in the dopamine D4 receptor. Biochem. 37, 15726–15736.

Padovani, A., Cosseddu, M., Premi, E., Archetti, S., Papetti, A., Agosti, C., Bigni, B., Cerini, C., Paghera, B., Bellelli, G., Borroni, B., 2010. The speech and language FOXP2 gene modulates the phenotype of frontotemporal lobar degeneration. J. Alzheimers Dis. 22, 923–931.

Paternico, D., Manes, M., Premi, E., Cosseddu, M., Gazzina, S., Alberici, A., Archetti, S., Bonomi, E., Cotelli, M.S., Cotelli, M., Turla, M., Micheli, A., Gasparotti, R., Padovani, A., Borroni, B., 2016. Frontotemporal dementia and language networks: cortical thickness reduction is driven by dyslexia susceptibility genes. Sci. Rep. 6, 30848.

Perry, D.C., Brown, J.A., Possin, K.L., Datta, S., Trujillo, A., Radke, A., Karydas, A., Kornak, J., Sias, A.C., Rabinovici, G.D., Gorno-Tempini, M.L., Boxer, A.L., De May, M., Rankin, K., Sturm, V.E., Lee, S.E., Matthews, B.R., Kao, A.W., Vossel, K.A., Tartaglia, M.C., Miller, Z.A., Seo, S.W., Sidhu, M., Gaus, S.E., Nana, A.L., Vargas, J.N.S., Hwang, J.-H.L., Ossenkoppele, R., Brown, A.B., Huang, E.J., Coppola, G., Rosen, H.J., Geschwind, D., Trojanowski, J.Q., Grinberg, L.T., Kramer, J., Miller, B.L., Seeley, W.W., 2017. Clinicopathological correlations in behavioural variant frontotemporal dementia. Brain 140, 3329–3345.

Piomelli, D., Pilon, C., Giros, B., Sokoloff, P., Martres, M.-P., Schwartz, J.-C., 1991. Dopamine activation of the arachidonic acid cascade as a basis for D1/D2 receptor synergism. Nature 353, 164–167.

Raj, A., Kuceyeski, A., Weiner, M., 2012. A network diffusion model of disease progression in dementia. Neuron 73, 1204–1215.

Ridgway, G.R., Omar, R., Ourselin, S., Hill, D.L., Warren, J.D., Fox, N.C., 2009. Issues with threshold masking in voxel-based morphometry of atrophied brains. NeuroImage 44, 99–111.

Rondou, P., Haegeman, G., Van Craenenbroeck, K., 2010. The dopamine D4 receptor: biochemical and signalling properties. Cell. Mol. Life Sci. 67, 1971–1986.

Rosen, H.J., Gorno-Tempini, M.L., Goldman, W.P., Perry, R.J., Schuff, N., Weiner, M., Feiwell, R., Kramer, J.H., Miller, B.L., 2002. Patterns of brain atrophy in frontotemporal dementia and semantic dementia. Neurology 58, 198–208.

Seeley, W.W., 2017. Mapping neurodegenerative disease onset and progression. Cold Spring Harb. Perspect. Biol. 9, 1–18.

Seeley, W.W., Menon, V., Schatzberg, A.F., Keller, J., Glover, G.H., Kenna, H., Reiss, A.L., Grecius, M.D., 2007. Dissociable intrinsic connectivity networks for salience processing and executive control. J. Neurosci. 27, 2349–2356.

Seeley, W.W., Crawford, R.K., Zhou, J., Miller, B.L., Grecius, M.D., 2009. Neurodegenerative diseases target large-scale human brain networks. Neuron. 62, 42–52.

Shi, Y., Yamada, K., Liddelow, S.A., Smith, S.T., Zhao, L., Leo, W., Tsai, R.M., Spina, S., Grinberg, L.T., Rojas, J.C., Gallardo, G., Wang, K., Roh, J., Robinson, G., Finn, M.B., Jiang, H., Sullivan, P.M., Baufield, C., Wood, M.W., Sutphen, C., McCue, L., Xiong, C., Del-Aguila, J.L., Morris, J.C., Cruchaga, C., Fagan, A.M., Miller, B.L., Boxer, A.L., Seeley, W.W., Butovsky, O., Barres, B.A., Paul, S.M., Holtzman, D.M., 2017. ApoE4 markedly exacerbates tau-mediated neurodegeneration in a mouse model of tauopathy. Nature 549, 523–529.

Sturm, V.E., Solberger, M., Seeley, W.W., Rankin, K.P., Ascher, E.A., Rosen, H.J., Miller, B.L., Levenson, R.W., 2013. Role of right pregenual anterior cingulate cortex in self-conscious emotional reactivity. Scan 8, 468–474.

Svingos, A.L., Periasamy, S., Pickel, V.M., 2000. Presynaptic dopamine D(4) receptor localization in the rat nucleus accumbens shell. Synapse. 36, 222–232.

Tarazi, F.I., Baldessarini, R.J., 1999. Dopamine D_4 receptors: significance for molecular psychiatry at the millennium. Mol. Psychiatry 4, 529–538.

Van Tol, H.H.M., Wu, C.M., Guan, H.-C., Ohara, K., Bunzow, J.R., Civelli, O., Kennedy, J., Seeman, P., Niznik, H.B., Jovanovic, V., 1992. Multiple dopamine D4 receptor variants in the human population. Nature. 358, 149–152.

Wang, E., Ding, Y.-C., Flodman, P., Kidd, J.R., Kidd, K.K., Grady, D.L., Ryder, O.A., Spence, M.A., Swanson, J.M., Moyzis, R.K., 2004. The genetic architecture of selection at the human dopamine receptor D4 (DRD4) gene locus. Am. J. Hum. Genet. 74, 931–944.

Warren, J.D., Rohrer, J.D., Schott, J.M., Fox, N.C., Hardy, J., Rossor, M.N., 2013. Molecular nexopathies: a new paradigm of neurodegenerative disease. Trends Neurosci. 36, 561–569.

Yan, Y., Pushparaj, A., Le Strat, Y., Gamaleddin, I., Barnes, C., Justinova, Z., Goldberg, S.R., Le Foll, B., 2012. Blockade of dopamine D4 receptors attenuates reinstatement of extinguished nicotine-seeking behavior. Neuropsychopharmacology 37, 685–696.

Zhou, J., Gennatas, E.D., Kramer, J.H., Miller, B.L., Seeley, W.W., 2012. Predicting regional neurodegeneration from the healthy brain functional connectome. Neuron. 73, 1216–1227.